



Open Access: ISSN 1847-9286

<https://pub.iapchem.org/ojs/index.php/JESE>

Original scientific paper

## Mild steel corrosion inhibition by 7-(ethylthiobenzimidazolyl) theophylline

N'guessan Yao Silvère Diki<sup>1,✉</sup>, Nagnonta Hippolyte Coulibaly<sup>2</sup>, Kadjo François Kassi<sup>3</sup> and Albert Trokourey<sup>1</sup>

<sup>1</sup>Laboratoire de Constitution et Réaction de la Matière, UFR SSMT, Université Félix Houphouët-Boigny, 22 BP 582 Abidjan 22, Côte d'Ivoire

<sup>2</sup>UFR Sciences et Technologies, Université de Man, BP 20 Man, Côte d'Ivoire

<sup>3</sup>Laboratoire de Thermodynamique et de Physico-Chimie du Milieu, UFR SFA, UNA, Côte d'Ivoire

Corresponding author: ✉[dickiensil2@gmail.com](mailto:dickiensil2@gmail.com)

Received: January 11, 2021; Revised: April 3, 2021; Accepted: April 7, 2021

### Abstract

The corrosion inhibition of mild steel by 7-(ethylthiobenzimidazolyl) theophylline (7-ETBT) in 1 M HCl medium was investigated through weight loss and Tafel polarization techniques within a temperature range of 298 to 318 K. The inhibition efficiency depends on the concentration of 7-ETBT and reaction system temperature. The maximum inhibition efficiency values of 90.73 and 87.06 %, respectively, were estimated using both weight loss and Tafel polarization techniques at 298 K. The results suggest spontaneous and predominant physical adsorption of 7-ETBT on the metal surface which obeys Langmuir isotherm model. Furthermore, Tafel polarization method revealed that 7-ETBT is a mixed-type inhibitor. Potentiodynamic polarization results are in accordance with weight loss data to a good extent.

### Keywords

Organic inhibitor; inhibition efficiency; weight loss, Tafel polarization; physical adsorption

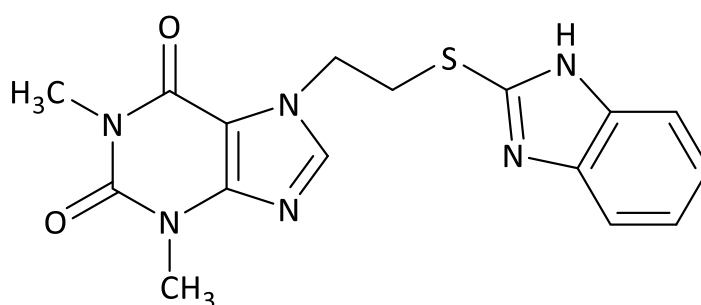
### Introduction

Corrosion of metallic materials in acidic solution is of huge concern and its inhibition has been deeply investigated [1,2]. Hydrochloric acid is widely used in various technological processes in industry including pickling baths, extraction and processing of oil and gas and in other chemical and petrochemical industries [3,4]. Corrosion of mild steel is important and expensive problem in the industries and represents a significant portion of losses as a result of lost production, inefficient operation, and high maintenance cost. It has been found that one of the best methods for protecting metals against corrosion involves the use of inhibitors which are mostly organic compounds. Organic

compounds contain electronegative functional groups and  $\pi$ -electrons in triple or conjugated double bonds that slow down the corrosion rate [5-7].

Many organic compounds have been investigated as corrosion inhibitors for different types of metals including mild steel [8-10]. With increased awareness towards environmental pollution and control, the search for less toxic and environmentally friendly corrosion inhibitors is becoming increasingly important. Thus, researchers have focused their works on several synthesized compounds, for which non-toxicity tests are carried out during their synthesis [11-14].

A detailed literature review showed no data available regarding the behavior of 7-ETBT as corrosion inhibitor for mild steel. Herein, for the first time, we report the use of 7-ETBT as a corrosion inhibitor for mild steel in one molar hydrochloric acid medium. The aim of the present paper is to evaluate the behavior of the studied inhibitor against mild steel corrosion in 1M HCl, by analyzing both thermodynamic data and potentiodynamic polarization parameters. The chemical structure of 7-ETBT is shown in Scheme 1.



**Scheme 1.** Chemical structure of 7-(ethylthiobenzimidazolyl) theophylline

## Experimental

### Mild steel specimen and reagents

The test samples used in corrosion studies were cut from a piece of mild steel into coupons of dimensions 1×1×1 cm. Mild steel was of the following chemical composition (wt.%) (C: 0.17, Mn: 0.03, Si: 0.14, S: 0.028, P: 0.033 and Fe: balance).

7-ETBT, a beige color chemical with molecular formula  $C_{16}H_{16}N_6O_2S$ , was provided by the Laboratory of Organic Chemistry and Natural Substances, Felix Houphouet-Boigny University. Its molecular structure was identified by  $^1H$  NMR and  $^{13}C$  NMR spectroscopy:

-RMN  $^1H$  (400 MHz, DMSO- $d_6$ ,  $\delta$  / ppm): 3.22 (s, 6H,  $-CH_3-$ ); 3.74 (dd,  $J=6.6, 5.1$  Hz, 2H, N- $CH_2-$ ); 4.60 (dd, 2H,  $-CH_2-S$ ); 7.04 (dd, 2H,  $H_{Ar}$ ); 7.32 (dd, 2H,  $H_{Ar}$ ); 7.96 (s, 1H, N=CH-).

-RMN  $^{13}C$  (DMSO,  $\delta$  / ppm): = 27.56 ( $CH_3-$ ); 29.22 ( $CH_3-$ ); 32.00 (N- $CH_2-$ ); 46.49 ( $-CH_2-S$ ); 150 ( $C_{Ar}$ ); 149.34 ( $C_{Ar}$ ); 148.34 ( $C_{Ar}$ ).

The corrosive aqueous solution of 1 M HCl was prepared by dilution of analytical grade 37 % HCl purchased from Sigma-Aldrich Chemicals with bi-distilled water. Acetone of purity 99.5 % was also purchased from Sigma-Aldrich Chemicals. 1 M HCl solutions without or with different quantities of 7-ETBT, ranging from 0.02 to 2 mM were then prepared.

### Weight loss measurements

Each test was conducted in 50 mL of aerated and unstirred 1 M HCl solution without or with desired concentrations of the tested inhibitor for 1 h immersion time at different temperatures. Temperature was regulated by a water-controlled thermostat (Memmert, precision  $\pm 0.5$  °C). Prior experiments, mild steel coupons were polished with different emery papers, washed thoroughly

with bi-distilled water, degreased and dried with acetone. The obtained samples were then kept in an oven (Memmert) at 70 °C and weighed accurately. After 1 h of immersion in the corrosive media with or without 7-ETBT, the specimens were carefully washed in bi-distilled water, dried and reweighed accurately. Triplicate experiments were performed in each case and the mean value of the weight loss was reported. From the weight loss measurements, the corrosion rate ( $CR$ ), degree of surface coverage ( $\theta$ ), and inhibition efficiency ( $IE$ ) were calculated using following equations [15]:

$$CR = \frac{\Delta m}{St} \quad (1)$$

$$\theta = \frac{CR_0 - CR}{CR_0} \quad (2)$$

$$IE = \left( \frac{CR_0 - CR}{CR_0} \right) 100 \quad (3)$$

where  $CR_0$  and  $CR$  (expressed in  $\text{mg h}^{-1} \text{cm}^{-2}$ ) are respectively corrosion rate without and with 7-ETBT,  $\Delta m$  is weight loss,  $S$  is total surface of steel specimen and  $t$  is immersion time.

### *Electrochemical measurements*

Electrochemical experiments were carried out at the ambient temperature (298 K) in a conventional three-electrode glass cell of 100 mL cell capacity. Mild steel specimen served as the working electrode (WE) having the exposed surface of  $1.000 \pm 0.001 \text{ cm}^2$ , with the rest being covered by a commercially available polymeric resin. A platinum electrode and a saturated calomel electrode (SCE) coupled to a fine Luggin capillary served as the counter (CE) and reference (RE) electrode, respectively. All potential values given in this study are referred to SCE reference. Solutions were aerated, unstirred and prepared like these used for weight loss measurements. All measurements were performed with the Autolab PGSTAT 20 potentiostat (Ecochemie, Utrecht Netherlands) controlled by GPES 4.4 software. Origin 6.0 software was used for plotting, graphing and fitting data. Before each measurement, the mild steel working electrode was prepared as described for weight loss measurements and immersed in the test solution for 30 min to establish steady state at the open circuit potential ( $E_{\text{ocp}}$ ). Tafel polarization curves were carried out by linear potential sweeps at the scan rate of 1 mV/s, applied from the cathodic potential of  $-1000 \text{ mV}$  to anodic potential of  $+1000 \text{ mV}$  with respect to  $E_{\text{ocp}}$ . Each experiment was repeated at least three times using always a fresh mild steel electrode. Only well reproducible results were reported. The inhibition efficiency ( $IE$ ) was calculated according to:

$$IE = \left( \frac{j_{\text{corr}}^0 - j_{\text{corr}}^{\text{inh}}}{j_{\text{corr}}^0} \right) 100 \quad (4)$$

where  $j_{\text{corr}}^0$  and  $j_{\text{corr}}^{\text{inh}}$  are referred to the corrosion current density in solutions without and with the inhibitor, respectively.

## **Results and discussion**

### *Weight loss measurement*

The weight loss method has found broad practical application. A major advantage of this method is its relative simplicity and availability. In addition, this method uses a direct parameter for the quantitative evaluation of corrosion, the loss in weight of the metal [16]. The data obtained from weight loss measurements for the corrosion rates of mild steel samples in 1M HCl solutions with and without 7-ETBT at different temperatures are presented in Figures 1 and 2.

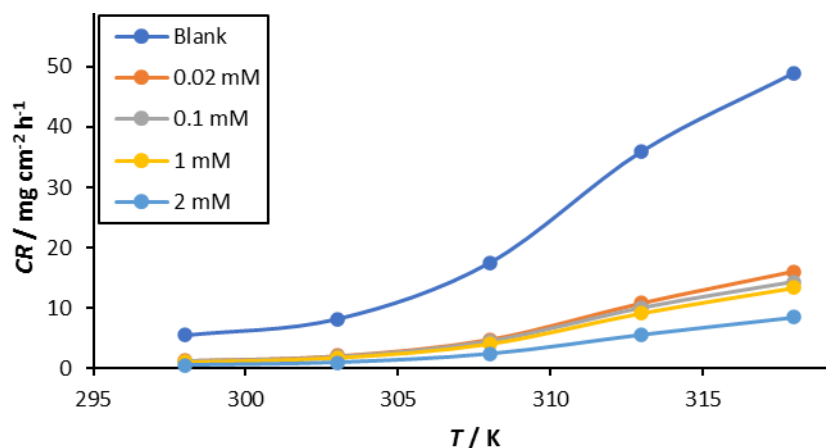


**Figure 1.** Evolution of corrosion rate of mild steel with temperature at different concentrations of 7-ETBT

As displayed in Figure 1, the curves showed that corrosion rate of mild steel in the studied medium increases with increasing temperature. However, the increase in 7-ETBT concentration (from 0.02 to 2 mM) is accompanied by decrease of corrosion rate over the temperature range (298-318 K). These results highlight the fact that adsorption of inhibitor on the metallic surface increases with increase in inhibitor concentration. The evolution of inhibition efficiency calculated using equation (3) versus temperature is illustrated in Figure 2.

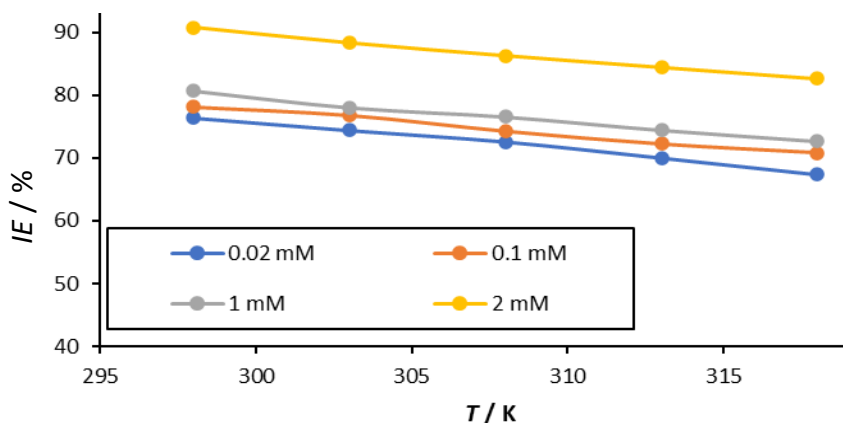


**Figure 2.** Inhibition efficiency vs. temperature for different concentrations of 7-ETBT

As shown in Figure 2, the inhibition efficiency decreases with the rise in temperature for the inhibitor concentration range studied. According to the literature [17], the decrease in inhibition efficiency with increase of temperature indicates that the process of adsorption of the inhibitor on the corroding metal surface is physisorption. This effect can be also attributed to the increase in the solubility of the protective films and of any reaction products precipitated on the surface of the metal [18], thereby increasing the metal surface exposure to corrosive attack when the temperature rises. All these observations indicate that the studied inhibitor acts as an effective inhibitor of mild steel corrosion over the concentration range studied. This behavior could be explained by the formation of a barrier which separates the metal from the acidic solution.

#### Adsorption considerations

Attempts were made to fit degree of surface coverage ( $\theta$ ) values to three isotherms including Langmuir, El-Awady and Flory-Huggins. The best fit according to the strong correlation ( $R^2 > 0.995$ ) and slopes of straight lines close to unity over the temperature range studied were obtained with Langmuir adsorption model. In the rearranged form, Langmuir adsorption isotherm is expressed as:

$$\frac{C_{\text{inh}}}{\theta} = \frac{1}{K_{\text{ads}}} + C_{\text{inh}} \quad (5)$$

where  $K_{\text{ads}}$  is adsorption equilibrium constant.

The curve of  $C_{\text{inh}}/\theta$  as a function of  $C_{\text{inh}}$  (inhibitor concentration) is shown in Figure 3.

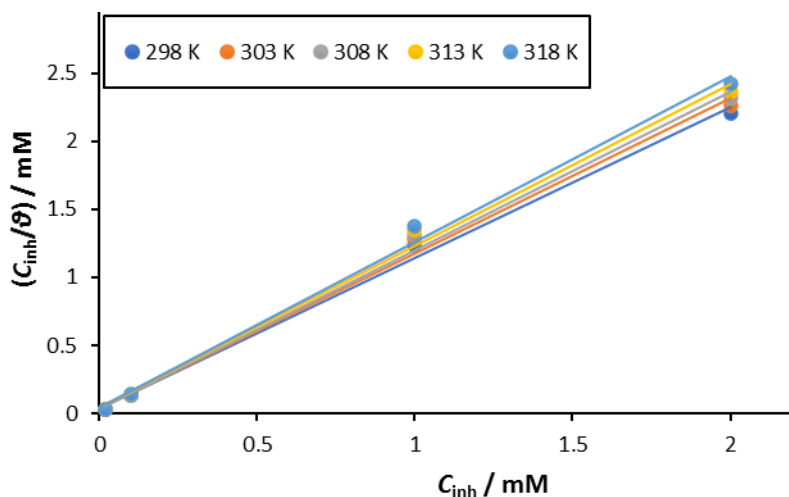


**Figure 3.** Langmuir adsorption isotherm for 7-ETBT on mild steel in 1M HCl at different temperatures

Regression parameters related to Langmuir adsorption isotherm are gathered in Table 1.

**Table 1.** Regression parameters of Langmuir adsorption isotherm of 7-ETBT on mild steel surface in 1 M HCl

$T / K$	$R^2$	Slope	Intercept
298	0.9960	1.1080	0.0351
303	0.9955	1.1396	0.0370
308	0.9958	1.1653	0.0376
313	0.9953	1.1911	0.0407
318	0.9951	1.2171	0.0424

In order to assess the strength of interactions between inhibitor molecules and the metal surface, the values of adsorption equilibrium constant  $K_{\text{ads}}$  were calculated using intercepts of straight lines on  $C_{\text{inh}}/\theta$ -axis. The calculated adsorption equilibrium constant was related to the standard free energy of adsorption  $\Delta G^0_{\text{ads}}$  by the following equation [19]:

$$\Delta G^0_{\text{ads}} = -RT \ln (55.5 K_{\text{ads}}) \quad (6)$$

In equation (6) [20], 55.5 is concentration of water in  $\text{mol L}^{-1}$ ,  $T$  is absolute temperature while  $R$  is universal gas constant. The values of  $\Delta G^0_{\text{ads}}$  and other adsorption thermodynamic functions are summarized in Table 2.

**Table 2.** Adsorption thermodynamic functions of 7-ETBT on mild steel surface in 1M HCl

$T / K$	$K_{\text{ads}} / \text{M}^{-1}$	$\Delta G^0_{\text{ads}} / \text{kJ mol}^{-1}$	$\Delta H^0_{\text{ads}} / \text{kJ mol}^{-1}$	$\Delta S^0_{\text{ads}} / \text{kJ mol}^{-1}$
298	28490.03	-35.35		
303	27027.03	-35.81		
308	26595.74	-36.36	-7.52	93.40
313	24570.02	-36.74		
318	23584.91	-37.22		

In our work, the computed values of  $\Delta G^0_{\text{ads}}$  for 7-ETBT were ranging from  $-35.35$  to  $-37.22 \text{ kJ mol}^{-1}$  which indicated that adsorption of 7-ETBT on the mild steel surface may involve physisorption as well as chemisorption [21,22]. Decrease in values of  $K_{\text{ads}}$  with increasing temperature suggest that

desorption process is enhanced with increase in temperature [22]. The large negative values of  $\Delta G^0_{ads}$  reveal that the adsorption process occurs spontaneously and the adsorbed layer on the metallic surface is highly stable [23]. The standard adsorption enthalpy change ( $\Delta H^0_{ads}$ ) and the standard adsorption entropy change ( $\Delta S^0_{ads}$ ) are correlated with the standard Gibbs free energy ( $\Delta G^0_{ads}$ ) according to the following equation:

$$\Delta G^0_{ads} = \Delta H^0_{ads} - T\Delta S^0_{ads} \tag{7}$$

Figure 4 presents plots of  $\Delta G^0_{ads}$  versus temperature. The values of  $\Delta H^0_{ads}$  and  $\Delta S^0_{ads}$  obtained by linear regression are listed in Table 2.  $\Delta H^0_{ads}$  value is negative, showing an exothermic process. According to the literature [24], an exothermic process means either physisorption or chemisorption. Therefore this result confirms that the process of adsorption is both physisorption and chemisorption [25].  $\Delta S^0_{ads}$  value is positive, meaning that disorder increases during the adsorption process. This situation can be explained by the desorption of water molecules replaced by the inhibitor.

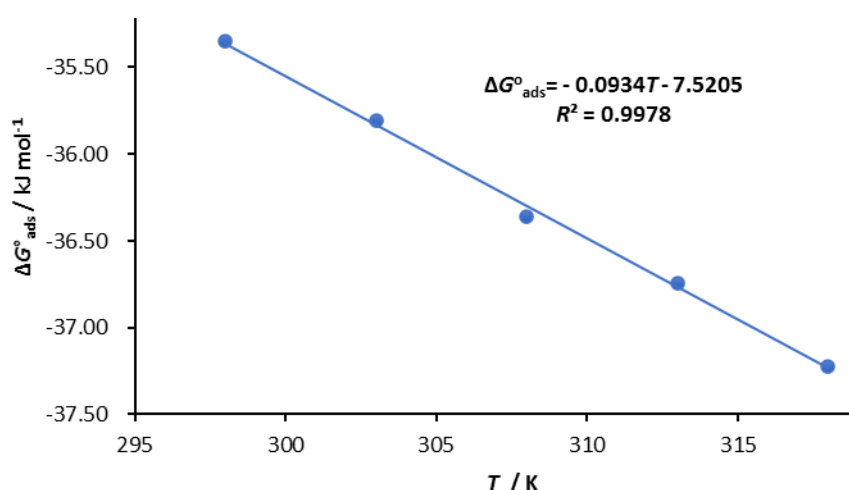


Figure 4.  $\Delta G^0_{ads}$  vs. temperature for adsorption of 7-ETBT on mild steel in 1 M HCl

Effect of temperature and activation parameters of the corrosion process

The activation energy ( $E_a$ ) can be calculated by using Arrhenius equation:

$$\log(CR) = \log A - \frac{E_a}{2.303RT} \tag{8}$$

where A is the Arrhenius pre-exponential constant.

Plot of  $\log CR$  versus  $1/T$  yields a straight line (Figure 5), where slope and intercept define  $E_a / 2.303 R$  and  $\log A$  values, respectively.

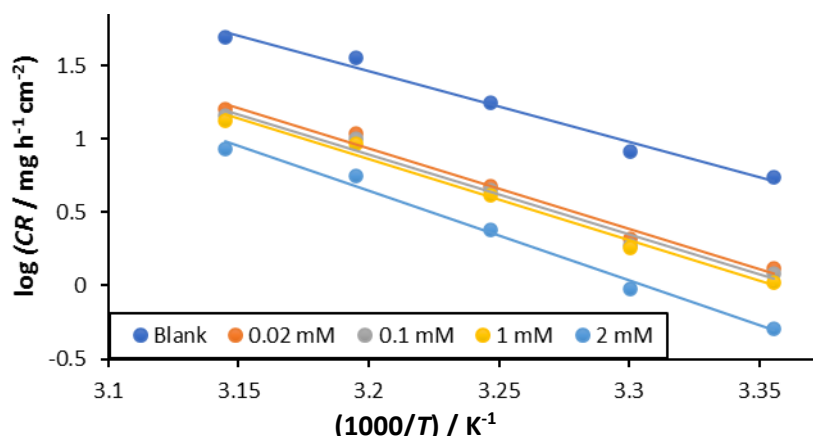


Figure 5. Arrhenius plots for mild steel corrosion in 1 M HCl without and with of 7-ETBT

The other activation parameters for the corrosion process were calculated from the Arrhenius equation:

$$\log\left(\frac{CR}{T}\right) = \left[ \log\left(\frac{R}{N h}\right) + \frac{\Delta S_a^*}{2.303 R} \right] - \frac{\Delta H_a^*}{2.303 RT} \quad (9)$$

where  $\Delta S_a^*$  is the change in apparent activation entropy,  $\Delta H_a^*$  is the change in apparent activation enthalpy,  $N$  is Avogadro number and  $h$  is Planck constant.

Figure 6 presents plots  $\log (CR/T)$  versus  $1/T$  for mild steel corrosion in blank solution and solutions with different concentrations of 7-ETBT. The slope  $-\Delta H_a^* / 2.303RT$  and the intercept  $(\log (R / N h) + \Delta S_a^* / 2.303 R)$  of each straight-line lead to the values of activation enthalpy change and activation entropy change (Table 3).

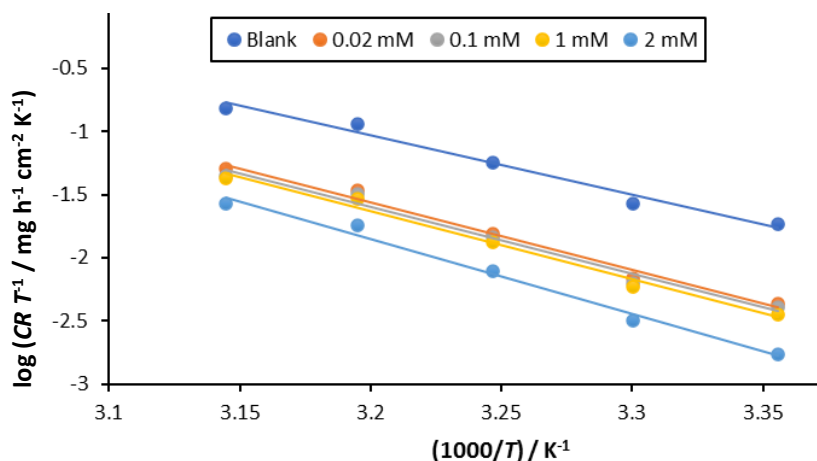


**Figure 6.** Transition state plots for mild steel corrosion in 1 M HCl without and with 7-ETBT

**Table 3.** Activation parameters for mild steel corrosion in 1 M HCl without and with 7-ETBT

Solution concentration, mM	$E_a / \text{kJ mol}^{-1}$	$\Delta H_a^* / \text{kJ mol}^{-1}$	$\Delta S_a^* / \text{J mol}^{-1} \text{K}^{-1}$
0.0 (blank)	92.23	92.57	69.66
0.02	104.27	101.58	97.31
0.10	104.90	102.21	100.08
1.00	105.68	102.99	101.19
2.00	116.52	113.81	131.62

From Table 3, it seems that  $E_a$  and  $\Delta H_a^*$  values are varied in the same manner, *i.e.* they increase with increase of inhibitor concentration, what is probably due to the thermodynamic relation between them ( $\Delta H_a^* = E_a - RT$ ). Also, it can be seen that the values of  $E_a$  are higher in inhibited than uninhibited (blank) solutions. On the other hand, higher values of  $E_a$  in the presence of inhibitor compared to that in its absence, and decrease of the inhibition efficiency ( $IE$ ) with increase in temperature can be interpreted as an indication of predominant physical adsorption process [26-28]. Moreover, the positive signs of  $\Delta H_a^*$  reflect the endothermic effect of mild steel dissolution process. The value of  $\Delta S_a^*$  is also higher for inhibited than uninhibited solutions. This phenomenon shows that disorder increases on going from reactant to activated complex. This might be the result of the adsorption of organic inhibitor molecules from the acidic solution which could be regarded as a quasi-substitution process between the organic compound in the aqueous phase and water molecules at the metal surface [29].

#### Tafel polarization

Potentiodynamic polarization curves were recorded to obtain information about the influence of 7-ETBT on anodic and cathodic processes at mild steel in the test solution. Polarization curves for

mild steel in 1 M HCl without and with 7-ETBT at different concentrations are shown in Figure 7. The anodic and cathodic current–potential curves were extrapolated up to their intersection points, where corrosion current density ( $j_{\text{corr}}$ ) and corrosion potential ( $E_{\text{corr}}$ ) are evaluated. The effect of increasing concentration of 7-ETBT on the anodic and cathodic polarization curves of mild steel in 1 M HCl solution at 298 K is also presented in Figure 7. Increasing of 7-ETBT concentration moved both cathodic and anodic branches of polarization curves toward lower current densities, what reveals that inhibitor molecules are adsorbed on the metal surface.

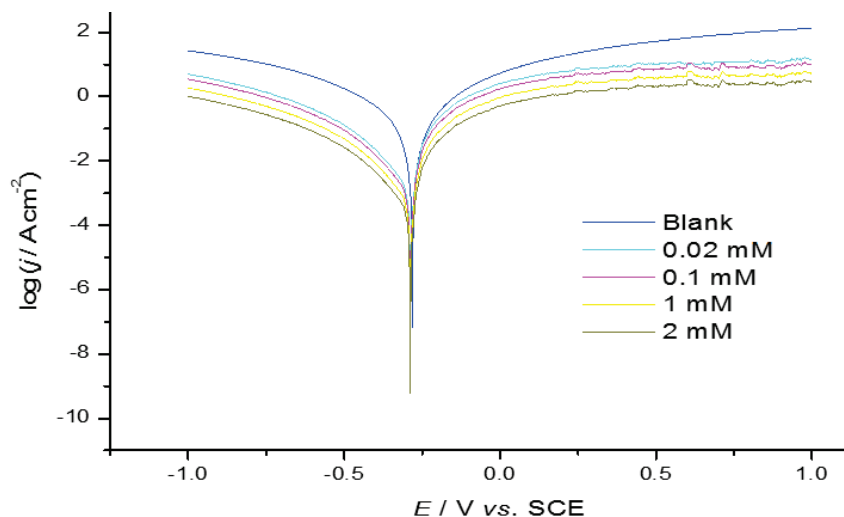


**Figure 7.** Potentiodynamic polarization curves obtained for mild steel in 1 M HCl at 298 K, without and with 7-ETBT

Electrochemical parameters associated with Tafel polarization measurements such as anodic and cathodic Tafel slopes ( $b_a$  and  $b_c$ ), corrosion potential ( $E_{\text{corr}}$ ) and corrosion current density ( $j_{\text{corr}}$ ) were estimated from polarization curves and listed in Table 4, together with  $IE$  values calculated using equation (4). As is presented in Table 4, the slopes of cathodic and anodic Tafel lines are almost constant and independent on the inhibitor concentration, meaning that the inhibiting action of the tested compound occurred by simple blocking of the available surface area. In other words, the inhibitor decreased the surface area available for anodic dissolution and hydrogen evolution reactions, without affecting their reaction mechanisms.

**Table 4.** Potentiodynamic polarization data for corrosion of mild steel in 1 M HCl solutions without and with different concentrations of 7-ETBT at 298 K

$C_{\text{inh}} / \text{mM}$	$E_{\text{corr}} / \text{mV vs. SCE}$	$j_{\text{corr}} / \mu\text{A cm}^{-2}$	$b_a / \text{mV dec}^{-1}$	$-b_c / \text{mV dec}^{-1}$	$IE / \%$
0 (blank)	-453.53	451.06	104.85	115.31	-
0.02	-469.42	135.05	108.13	164.02	70.06
0.1	-470.30	116.84	117.52	159.60	74.10
1	-472.61	94.81	121.93	168.38	78.98
2	-482.68	58.35	129.80	172.29	87.06

## Conclusions

From the results of the present study, it can be concluded that 7-ETBT is the efficient corrosion inhibitor of mild steel in 1 M HCl, reaching the inhibition efficiency of almost 90 % for 2 mM of 7-ETBT at 298 K.

The inhibition efficiency of 7-ETBT is concentration and temperature dependent. Inhibition efficiency increases with increase of inhibitor concentration (0.02-2 mM) and decrease of

temperature. Decrease of inhibition efficiency with increase of temperature (298-318 K) suggests physisorption of inhibitor molecules at the metal surface. In addition, the values of free energy of adsorption suggest both physisorption and chemisorption mechanisms with a predominant physisorption effect. The obtained data fit well the Langmuir adsorption isotherm.

Potentiodynamic polarization data reveal that the studied inhibitor is a mixed-type one, and its inhibiting action is occurring by simple blocking of the available surface area. In general, Tafel polarization data confirm the results obtained from weight loss study.

## References

- [1] I. B. Obot, S. A. Umoren, N. O. Obi-Egbedi, *Journal of Materials and Environmental Science* **2** (2011) 60-71.
- [2] G. Karthik, M. Sundaravadivelu, *Egyptian Journal of Petroleum* **25(2)** (2016) 183-191 <https://doi.org/10.1016/j.ejpe.2015.04.003>.
- [3] I. Nadi, Z. Belattmania, B. Sabour, A. Reani, A. Sahibed-dine, C. Jama, F. Bentiss, *International Journal of Biological Macromolecules* **141** (2019) 137-149 <https://doi.org/10.1016/j.ijbiomac.2019.08.253>.
- [4] M. Madhumala, D. Madhavi, T. Sankarshana, S. Sridhar, *Journal of the Taiwan Institute of Chemical Engineers* **45(4)** (2014) 1249-1259 <https://doi.org/10.1016/j.jtice.2014.02.010>.
- [5] M. A. Quraishi, R. Sardar, *Corrosion* **58(9)** (2002) 748-755 <https://doi.org/10.5006/1.3277657>.
- [6] S. Aribi, S. J. Olusegun, G. L. S. Rodrigues, A. S. Ogunbadejo, B. Igbaroola, A. T. Alo, W.R. Rocha, N.D.S. Mohallem, P. A. Olubambi, *Journal of the Taiwan Institute of Chemical Engineers* **112** (2020) 222-231 <https://doi.org/10.1016/j.jtice.2020.06.011>.
- [7] G. Xu, K. Wang, X. Dong, L. Yang, M. Ebrahimi, H. Jiang, Q. Wang, W. Ding, *Journal of Materials Science & Technology* **71** (2021) 12-22 <https://doi.org/10.1016/j.jmst.2020.08.052>.
- [8] M. M. Antonijevic, M. B. Petrovic, *International Journal of Electrochemical Science* **3** (2008) 1-28.
- [9] S. Rajendran, S. Vaibhavi, N. Anthony, D. C. Trivedi, *Corrosion* **59** (2003) 529-534 <https://doi.org/10.5006/1.3277584>.
- [10] N. H. Coulibaly, Y. S. Brou, J. Creus, A. Trokourey, *Journal of Materials Science and Chemical Engineering* **6** (2018) 100-121 <https://doi.org/10.4236/msce.2018.63008>.
- [11] N. Y. S. Diki, G. G. D. Diomandé, S. J. Akpa, O. Ouédraogo, L. A. G. Pohan, P. M. Niamien, A. Trokourey, *International Journal of Applied Pharmaceutical Sciences and Research* **3(4)** (2018) 41-53 <https://doi.org/10.21477/ijapsr.3.4.1>.
- [12] A. D. Ehouman, G. G. D. Diomandé, P. M. Niamien, D. Sissouma, A. Trokourey, *IOSR Journal of Applied Chemistry* **9(10)** (2016) 17-25 <https://doi.org/10.9790/5736-0910011725>.
- [13] A. Ouédraogo, S. J. Akpa, N. Y. S. Diki, G. G. D. Diomandé, N. H. Coulibaly, A. Trokourey, *Journal of Materials Science and Chemical Engineering* **6** (2018) 31-49 <https://doi.org/10.4236/msce.2018.68004>.
- [14] D. Ehouman, J. S. Akpa, P. M. Niamien, D. Sissouma, A. Trokourey, *Der Pharma Chemica* **8(10)** (2016) 274-286.
- [15] K. F. Khaled, *International Journal of Electrochemical Science* **3** (2008) 462-475.
- [16] V. Kouakou, P. M. Niamien, A. J. Yapo, A. Trokourey, *Chemical Science Review and Letters* **5** (2016) 131-146.
- [17] R. Saratha R. Meenakshi, *Der Pharma Chemica* **2(1)** (2010) 287-294.
- [18] N. Santhini T. Jeyaraj, *Journal of Chemical and Pharmaceutical Research* **4** (2012) 3550-3556.
- [19] H. Keleş, M. Keleş, I. Dehri, O. Serindağ, *Colloids Surface A: Physicochemical and Engineering Aspects* **320** (2008) 138-145 <https://doi.org/10.1016/j.colsurfa.2008.01.040>.
- [20] R. F. V. Villamil, P. Corio, S. M. L. Agostinho, J.C. Rubim, *Journal of Electroanalytical Chemistry* **472(2)** (1999) 112-119 [https://doi.org/10.1016/S0022-0728\(99\)00267-3](https://doi.org/10.1016/S0022-0728(99)00267-3).
- [21] K. F. Khaled, N. Hackerman, *Electrochimica Acta* **49** (2004) 485-495 <https://doi.org/10.1016/j.electacta.2003.09.005>.
- [22] M. A. Quraishi, A. Singh, V. K. Singh, D. K. Yadav, A. K. Singh, *Materials Chemistry and Physics* **122(1)** (2010) 114-122 <https://doi.org/10.1016/j.matchemphys.2010.02.066>.

- [23] M. Scendo, M. Hepel, *Journal of Electroanalytical Chemistry* **613** (2008) 35-50 <https://doi.org/10.1016/j.jelechem.2007.10.014>.
- [24] W. Durnie, R. De Marco, A. Jefferson, B. Kinsella, *Journal of the Electrochemical Society* **146(5)** (1999) 1751-1756 <https://doi.org/10.1149/1.1391837>.
- [25] N. Y. S. Diki, G. K. Gbassi, A. Ouedraogo, M. Berte, A. Trokourey, *Journal of Electrochemical Science and Engineering* **8(4)** (2018) 303-320 <https://doi.org/10.5599/jese.585>.
- [26] S. A. Umoren, *Cellulose* **15(5)** (2008) 751-761 <https://doi.org/10.1007/s10570-008-9226-4>.
- [27] N. Chaubey, Savita, V. K. Singh, M. A. Quraishi, *Journal of The Association of Arab Universities for Basic and Applied Sciences* **22** (2017) 38-44 <https://doi.org/10.9790/5736-0910011725>.
- [28] N. Y. S. Diki, K. V. Bohoussou, M. G.-R. Kone, A. Ouedraogo, A. Trokourey, *IOSR Journal of Applied Chemistry* **11(4)** (2018) 24-36 <https://doi.org/10.9790/5736-1104012436>.
- [29] L. Afia, R. Salghi, A. Zarrouk, H. Zarrok, O. Benali, B. Hammouti, S. S. Al-Deyab, A. Chakir, L. Bazzi, *Portugaliae Electrochimica Acta* **30(4)** (2012) 267-279 <https://doi.org/10.4152/pea.201204267>.